Chapter 10

Cross-drainage and drop structures

10.1 Aqueducts and canal inlets and outlets

10.1.1 Introduction

The alignment of a canal invariably meets a number of natural streams (drains) and other structures such as roads and railways, and may sometimes have to cross valleys. Cross-drainage works are the structures which make such crossings possible. They are generally very costly, and should be avoided if possible by changing the canal alignment and/or by diverting the drains.

10.1.2 Aqueducts

An aqueduct is a cross-drainage structure constructed where the drainage flood level is below the bed of the canal. Small drains may be taken under the canal and banks by a concrete or masonry barrel (culvert), whereas in the case of stream crossings it may be economical to flume the canal over the stream (e.g. using a concrete trough, Fig. 10.1(a)).

When both canal and drain meet more or less at the same level the drain may be passed through an inverted siphon aqueduct (Fig. 10.1(d)) underneath the canal; the flow through the aqueduct here is always under pressure. If the drainage discharge is heavily silt laden a silt ejector should be provided at the upstream end of the siphon aqueduct; a trash rack is also essential if the stream carries floating debris which may otherwise choke the entrance to the aqueduct.

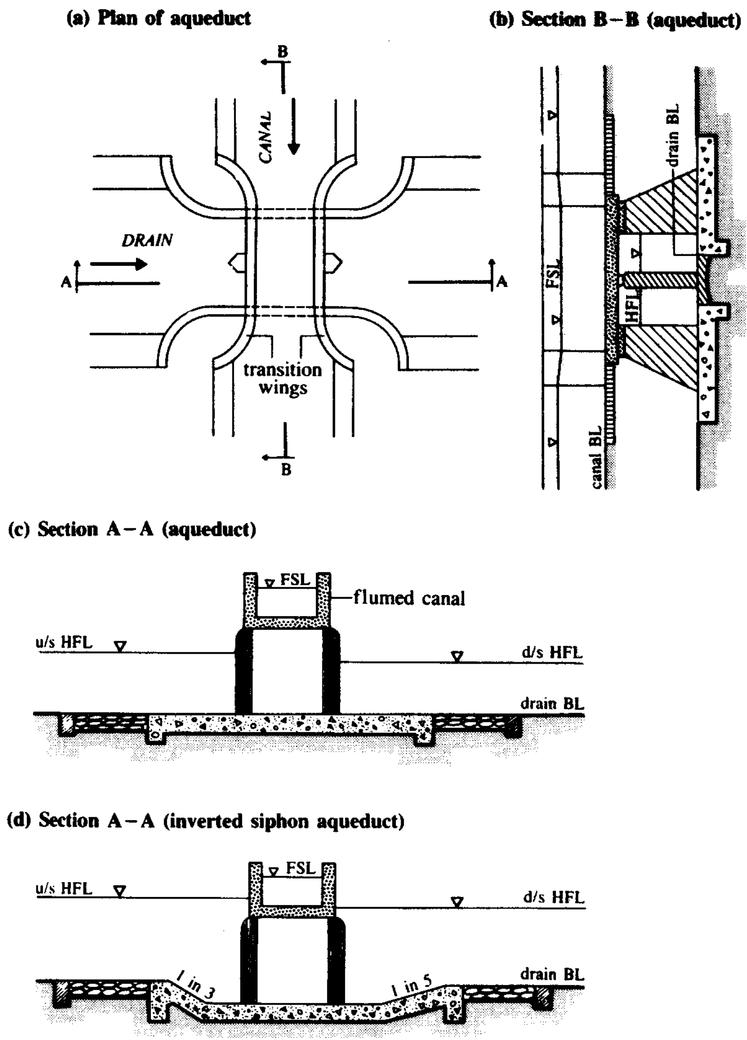

Fig. 10.1 Layout of an aqueduct

10.1.3 Superpassage

In this type of cross-drainage work, the natural drain runs above the canal, the canal under the drain always having a free surface flow. The superpassage is called a canal siphon or simply an inverted siphon if the canal bed under the drain is lowered to accommodate the canal flow, which will always be under pressure. The layouts of the superpassage and canal siphon are similar to those shown in Figs 10.1(a) and 10.1(b), with the canal and drain interchanged.

10.1.4 Level crossing

Level crossing facilities are provided when both the drain and the canal run at more or less the same level. This is more frequently used if either of the flows occurs for a short period (e.g. flash floods in the drain); in addition, the mixing of the two bodies of water must also be acceptable (quality considerations).

The plan layout of a level crossing with two sets of regulators, one across the drain and the other across the canal, is shown in Fig. 10.2. Normally, the canal regulator regulates its flow with the drain regulator kept closed. Whenever the flash floods occur, the canal gates are closed and drainage gates opened to let the flood flow pass.

10.1.5 Canal inlets and outlets

When the drainage flow is small it may be absorbed into the canal through inlets. The flow in the canal may be balanced, if necessary (in the case of small canals), by providing suitable outlets (or escapes). The inlet and outlet structures must also be provided with energy dissipators wherever necessary.

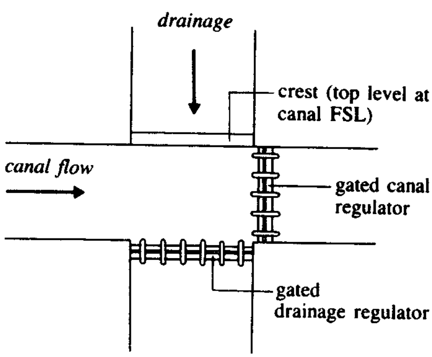

Fig. 10.2 Level crossing

The following worked example highlights the various aspects of the hydraulic design of a cross-drainage structure.

Worked Example 10.1

Design a siphon aqueduct for the following data:

	Canal	*Stream*
Discharge ($m^3 s^{-1}$)	30	500
Bed level (m AOD)	200.00	198.00
Canal FSL (m AOD)	202.00	
Bed width (m)	25.00	
Canal side slopes	1.5:1 V	
Stream HFL (m AOD)		200.50

The general terrain level is 200.00 m AOD.

Solution

DRAINAGE WATERWAY

Perimeter $P = 4.75Q^{1/2}$ (régime width, equation (9.9)) $\approx$ 106 m. Providing 12 piers of 1.25 m thickness, we have 13 spans of 7 m each. Therefore waterway provided $= 13 \times 7 + 12 \times 1.25 = 106$ m (satisfactory). Assuming a maximum velocity through the siphon barrels of $2\,\mathrm{m\,s^{-1}}$, height of barrel $= 500/(13 \times 7 \times 2) = 2.747$ m. Provide rectangular barrels, 7 m wide and 2.75 m high (shown in Fig. 10.5).

CANAL WATERWAY

Since the drainage width is large (106 m at the crossing) it is economical to flume (concrete, $n = 0.014$) the canal. Adopt a maximum flume ratio of 0.5. Therefore the flumed width of the canal (trough) $= 0.5 \times 25 = 12.5$ m. Providing a splay of 2:1 in contraction and a splay of 3:1 in expansion (Hinds, 1928),

$$\text{length of transitions in contraction} = 12.5\,\text{m},$$

$$\text{length of transitions in expansion} = 18.75\,\text{m}.$$

$$\text{The length of the trough from abutment to abutment} = 106\,\text{m}.$$

DESIGN OF FLUMED SECTION WITH TRANSITIONS

Referring to Fig. 10.3, the following results can be obtained to maintain a constant depth of flow of 2.0 m (given). The calculations are achieved from section 44 and proceed towards section 11 as tabulated below:

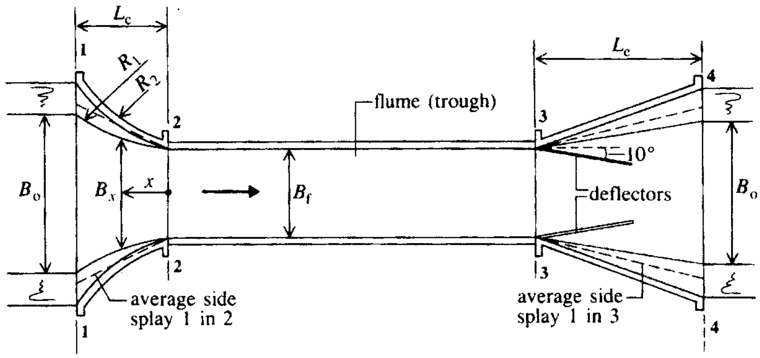

(L_c, L_e: contraction and expansion transition lengths. Length of deflector = ½ L_e; triangular wedge shaped with its height equal to u/s FSL)

Fig. 10.3 Transition with cylindrical inlet and linear outlet. L_c and L_e are contraction and expansion lengths

	Section			
	44	*33*	*22*	*11*
Width (m)	25.00	12.50	12.50	25.00
Area of flow (m^2)	56.00	25.00	25.00	56.00
Velocity ($m\,s^{-1}$)	0.536	1.20	1.20	0.536
Losses (m)		(expansion) 0.017	(friction) 0.017	(contraction) 0.012
Water surface level (m AOD)	202.000	201.959	201.976	202.406
Velocity head (m)	0.015	0.073	0.073	0.015
TEL (m AOD)	202.015	202.032	202.049	202.061
Flow depth (m)	2.00	2.00	2.00	2.00
Bed level (m AOD)	200.00	199.959	199.976	200.046

Note that the contraction loss $= 0.2(V_2^2 - V_1^2)/2g$; the expansion loss $= 0.3(V_3^2 - V_4^2)/2g$; the flume friction loss $= V_f^2 n^2 L_f / R_f^{4/3}$ (the suffix f denotes the flume, and o the original canal – $V_f = V_3 = V_2$; $V_o = V_4 = V_1$).

DESIGN OF TRANSITIONS

For a constant depth of flow the transition may be designed such that the rate of change of velocity per metre length of transition is constant. This approach yields the bed width of the transition at a distance x from the flume section as

$$B_x = B_o B_f L / [L B_o - (B_o - B_f)x]$$

which, modified after experimental studies (UPIRI, 1940), gives

$$x = LB_o^{3/2}[1 - (B_f/B_x)^{3/2}]/(B_o^{3/2} - B_f^{3/2})$$

where L is length of the transition.

The following table shows the calculated geometries of the transition provided:

B_x (m)	12.5	15.0	17.5	20.0	22.5	25.0	
x (m)	0	4.64	7.69	9.73	11.31	12.5	(contraction)
x (m)	0	6.96	11.53	14.59	16.96	18.75	(expansion)

The transitions are streamlined and warped to avoid any abrupt changes in the width.

Transitions with a cylindrical inlet with an average splay of 2:1 and a linear outlet with a splay of 3:1 provided with flow deflectors (Fig. 10.3; Ranga Raju, 1993) have been found to perform better than lengthy curved expansions.

As the flow is accelerating in a contracting transition and the energy loss is minimal any gradual contraction with a smooth and continuous boundary should be satisfactory, e.g. an elliptical quadrant is an alternative to a cylindrical quadrant for inlet transitions. The bedline profile for an elliptical quadrant transition has the equation

$$\left[\frac{x}{2(B_o - B_f)}\right]^2 + \left[\frac{y}{0.5(B_o - B_f)}\right]^2 = 1$$

and the length of transition given by

$$L_c = 2(B_o - B_f).$$

At any location (x) from flume end of the transition y is computed and the bed width B_x calculated by

$$B_x = B_o - 2y.$$

The side slope (m) of the transition ($m = 0$ for flume section and $m \geq 2$ for canal side slope) and bed elevation may be varied linearly along the transition length.

The expansion experiences considerable energy loss and care must be exercised in designing a hydraulically satisfactory transition.

On the basis of theoretical and experimental investigations Vittal and Chiranjeevi (1983) proposed the following design equations for bed width and the side slopes of an expanding transition. The bed widths B_x are fixed by

$$\frac{B_x - B_f}{B_0 - B_f} = \frac{x}{L}\left[1 - \left(\frac{1-x}{L}\right)^n\right]$$

where

$$n = 0.80 - 0.26 m_o^{1/2}$$

and the transition length, $L = 2.35(B_0 - B_f) + 1.65 m_o y_o$, y_o being the flow depth in the canal, and m_o its side slope. The side slopes (m) along the transition are given by

$$\frac{m}{m_o} = 1 - \left(1 - \frac{x}{L}\right)^{1/2}.$$

Using the constant specific energy condition in the transition between canal and flume the depth in the flume, y_f, and depths (y_x) along the transition length can be obtained. The energy balance between adjacent sections within the transition with expansion loss as $0.3(V_i^2 - V_{i+1}^2)/2g$ gives the bed elevations to be provided at successive sections so that the specific energy remains constant throughout the transition. Worked example 10.2 provides detailed design calculations for an expanding transition based on the Vittal and Chiranjeevi method.

WATER SURFACE PROFILE IN TRANSITION

The water surface in the transition may be assumed as two smooth parabolic curves (convex and concave) meeting tangentially. Referring to Fig. 10.4, the following equations give such profiles in transitions:

inlet transition, $y = 8.96 \times 10^{-4} x^2$;

outlet transition, $y = 2.33 \times 10^{-4} x^2$.

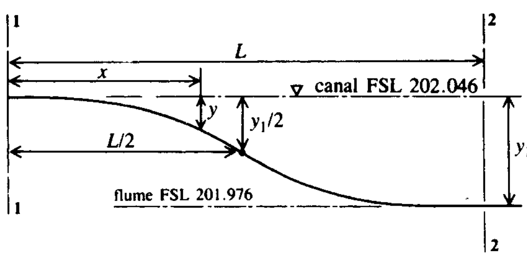

Fig. 10.4 Water surface profile in transition (inlet)

A highway 6 m wide is provided alongside the canal by dividing the flume into two compartments by a 0.3 m thick partition. The entire trough (flume section) can be designed as a monolithic concrete structure. Provide side walls and a bottom slab of about 0.4 m (to be fixed by the usual structural design methods).

SIPHON BARRELS

Thirteen barrels, each 7 m wide and 2.75 m high, are provided; assume that the effective roughness, $k = 0.6$ mm (concrete). The length of the barrel, $L = 12.50 + 0.30 + 2 \times 0.40 = 13.60$ m. The head loss through the barrel, $h_f = (1.5 + \lambda L/4R)V^2/2g$. The velocity through the barrel, $V = 500/(13 \times 7 \times 2.75) = 1.998\,\mathrm{m\,s^{-1}}$. The hydraulic radius, $R = 7 \times 2.75/\{2(7 + 2.75)\} = 0.987$ m. Therefore the Reynolds number $= 4VR/\nu = 8 \times 10^6$ and $k/4R = 1.5 \times 10^{-4}$. Hence, from Moody's chart, the friction factor $\lambda = 0.015$, giving $h_f = 0.316$ m. Therefore, the upstream HFL $= 200.500 + 0.316 = 200.816$ m AOD.

The uplift pressures on the roof of the barrel are as follows. The RL of the bottom of the trough $= 200.00 - 0.40 = 199.60$ m AOD. The entry loss at the barrel $= 0.5V^2/2g = 0.102$ m. Therefore the pressure head inside the barrel just downstream of its entry $= 200.816 - 0.102 - 199.600 = 1.114\,\mathrm{m} \simeq 11\,\mathrm{kN\,m^{-2}}$.

The most critical situation arises when the canal is empty and the siphon barrels are full. The weight of the roof slab $= 0.4 \times 2.4 \times 9.81 = 9.42\,\mathrm{kN\,m^{-2}}$ (assuming the relative density of concrete to be 2.4). Hence the roof slab needs additional reinforcement at its top to resist the unbalanced pressure forces (uplift pressures).

The total weight of the trough (when empty) needs to be checked against the total upward force and suitable anchorages to piers provided, if necessary. Equally, the trough floor slab has to be checked when it is carrying water at FSL and the level in the drainage is low, i.e. barrels running part full.

The uplift on the floor of the barrel (assuming the barrel floor thickness to be 1 m initially) is as follows:

RL of the bottom of the barrel $= 199.60 - 2.75 - 1.00 = 195.85$ m AOD;

RL of the drainage bed $= 198.00$ m AOD.

Therefore the static uplift on the floor $= 198.00 - 195.85 = 2.15$ m (the worst condition with the water table as the drain bed level). The seepage head (a maximum when the canal is at FSL and the drainage is empty) $= 202.00 - 198.00 = 4.00$ m.

In spite of the three-dimensional seepage flow pattern, Bligh's creep length may be approximated as follows. Creep flow commences from the beginning of the upstream transition (downstream of this the floor is impervious) and enters the first barrel floor; from its centre the flow follows downstream of the drain and emerges at the end of the impervious concrete floor of the barrel. Therefore the total creep length can be approximated as

> inlet transition length + $\frac{1}{2}$ barrel span + $\frac{1}{2}$ length of barrel impervious floor.

Let us assume that the total length of the impervious floor of the barrel is 25 m, consisting of the following:

length of barrel	= 13.60 m
pier projections, 2×0.8	= 1.60 m
downstream ramp (1:5), 1.15×5	= 5.75 m
upstream and downstream cut-offs, 2×0.3	= 0.60 m
total floor length	= 21.55 m

Therefore provide the upstream floor (1:3) length = 25.00 − 21.55 = 3.45 m. The total creep length = 12.5 + 7/2 + 25/2 = 28.5 m. The creep length up to the centre of the barrel = 12.5 + 7/2 = 16.0 m. Therefore the seepage head at the centre of the barrel = 4(1 − 16.0/28.5) = 1.75 m. The total uplift is then 2.15 + 1.75 = 3.90 m $\simeq$ 38 kN m^{-2}, and the weight of the floor = $1.00 \times 2.4 \times 9.81$ = 23.54 kN m^{-2}. Hence additional reinforcement has to be designed to resist the unbalanced uplift forces.

UPSTREAM AND DOWNSTREAM PROTECTION WORKS

The scour depth, R_s (regime scour depth, equation (9.10)) = $0.47(500/1)^{1/3}$ = 3.73 m. The upstream cut-off below HFL = $1.5R$ = 5.6 m. Therefore

$$\text{RL of upstream cut-off wall} = 200.816 - 5.60 = 195.00 \text{ (say) m AOD.}$$

The downstream cut-off below HFL = $1.75R_s$ = 6.53 m. Therefore

$$\begin{aligned} \text{RL of downstream cut-off wall} &= 200.50 - 6.53 = 194.00 \text{ (say) m AOD,} \\ \text{downstream apron length} &= 2.5(198.00 - 194.00) = 10\,\text{m}, \\ \text{upstream apron length} &= 2.0(198.00 - 195.00) = 6\,\text{m}. \end{aligned}$$

The detailed layout (longitudinal section) of the design is shown in Fig. 10.5.

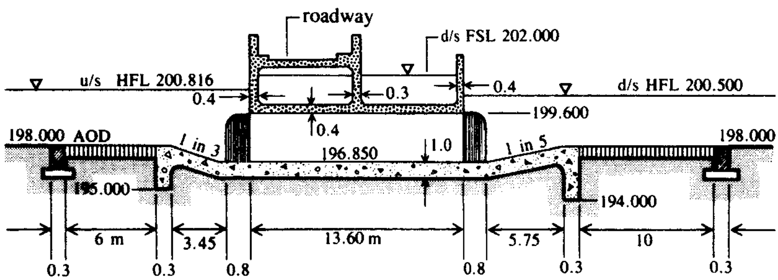

Fig. 10.5 Longitudinal section of the siphon aqueduct; all dimensions in metres

Worked Example 10.2

Design an expanding transition for the flume–canal layout of worked example 10.1 using the Vittal and Chiranjeevi (1983) method.

Solution

Design discharge = $30\,m^3\,s^{-1}$; bed width of canal, $B_o = 25$ m; bed width of flume, $B_f = 12.5$ m; side slope of canal, $m_o = 1.50$; bed level of canal = 200.00 m AOD; depth of flow in canal, $y_o = 2$ m (Worked example 10.1). Length of transition, $L = 2.35(25 - 12.5) + 1.65 \times 1.5 \times 2 \approx 36$ m. Bed width in transition, B_x, with $n = 0.8 - 0.26(1.5)^{1/2} = 0.482$,

$$B_x = 12.5 + (12.5x/36)[1 - (1 - x/36)^{0.482}].$$

Side slope in transition,

$$m = 1.5[1 - (1 - x/36)^{1/2}].$$

The complete set of calculations is presented in the table below:

Number	*Distance from upstream end of transition, x (m)*	*y_x (m)*	*m*	*B_x (m)*	*Δz (m)*	*Bed elevation (m AOD)*
1	36	2.000	1.50	25.000		200.000
2	27	1.985	0.75	17.069	0	200.000
3	18	1.965	0.44	15.737	0.001	199.999
4	9	1.950	0.20	12.545	0.002	199.998
5	0	1.935	0	12.500	0.003	199.997

10.2 Culverts, bridges and dips

10.2.1 Introduction

Highways cross natural drainage channels or canals, and provision must be made for appropriate cross-drainage works. The alignment of a highway along ridge lines (though it may be a circuitous route with less satisfactory gradients) may eliminate the cross-drainage work, thus achieving considerable savings.

Highway cross-drainage is provided by culverts, bridges and dips. Culverts are usually of shorter span (<6 m), with the top not normally forming part of the road surface like in a bridge structure. They are submerged structures buried under a high-level embankment. On the other hand, if the embankment is a low-level one, appropriate armouring protection works against overtopping during high floods have to be provided. Such a low-level structure (sometimes called a 'dip') in the absence of the culvert is often economical if the possible traffic delays do not warrant a costly high-level structure such as a bridge, keeping the road surface above all flood levels. A culvert combined with a dip (lowered road surface) is an attractive solution for small perennial streams with occasional flash floods; however, appropriate traffic warning systems/signs have to be incorporated.

Bridges are high-level crossing structures which can be expensive for large rivers. It is therefore essential to protect them even from rare floods. It is often advantageous to allow overtopping of part of the approach embankment, which may act as a fuse plug, to be replaced if necessary, after the flood event. Such an alternative route for the water avoids the overtopping of the bridge deck and, in addition, reduces the scouring velocities which may otherwise undermine the foundations of the structure.

10.2.2 Culverts

The culvert consists essentially of a pipe barrel (conveyance part) under the embankment fill, with protection works at its entrance and exit. At the entrance a head wall, with or without wing walls, and a debris barrier are normally provided. If necessary, an end wall with energy-dissipating devices is provided at the exit.

The culvert acts as a constriction and creates a backwater effect to the approach flow, causing a pondage of water above the culvert entrance. The flow within the barrel itself may have a free surface with subcritical or supercritical conditions depending on the length, roughness, gradient, and upstream and downstream water levels of the culvert. If the upstream head is sufficiently large the flow within the culvert may or may not fill the barrel, and its hydraulic performance depends upon the combination of entrance and friction losses, length of barrel, and the downstream backwater effects (Fig. 10.6).

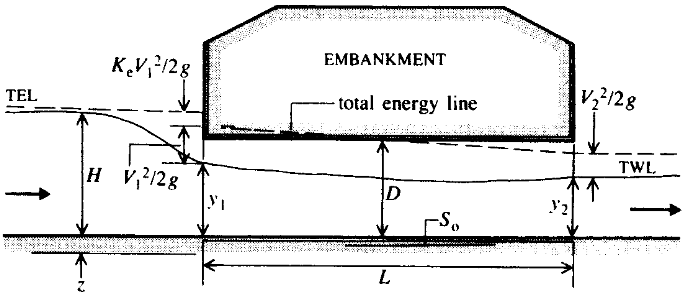

Fig. 10.6 Flow through a culvert

The various flow types that can exist in the pipe barrel of a culvert are shown in Table 10.1. The hydraulic design of the culvert is based on the characteristics of the barrel flow, and Worked examples 10.3 and 10.4 highlight calculations involving all the six types of flow listed in Table 10.1.

Table 10.1 Types of flow in the barrel of a culvert (Chow, 1983)

Type	*H/D*	*Exit depth* y_2	*Flow type*	*Length* L	*Slope* S_0	*Control*	*Remarks*
Submerged entrance conditions							
1	>1.0	>D	Full	Any	Any	Outlet	Pipe flow
2	>1.2	<D	Full	Long	Any	Outlet	Pipe flow
3	>1.2	<D	Part full	Short	Any	Outlet	Orifice
Free entrance conditions							
4	<1.2	<D >critical	Part full	Any	Mild	Outlet	Subcritical
5	<1.2	<D <critical	Part full	Any	Mlld	Outlet	Subcritical
6	<1.2	<D <critical	Part full	Any	Steep	Inlet	Supercritical
		>critical	Formation of hydraulic jump in barrel				

The reader is referred to Ramsbottom *et al.* (1997), Chanson (1999) and Mays (1999) for additional information on culvert flows, establishment of stage–discharge relationships and culvert design in general. Charbeneau *et al.* (2006) use a two parameter model describing the hydraulic performance of highway culverts operating under inlet control for both unsubmerged and submerged conditions.

The hydraulic performance of a culvert can be improved by the adoption of the following guidelines.

(a) Culvert alignment

As a general rule, the barrel should follow the natural drainage alignment and its gradient, in order to minimize head losses and erosion. This may lead to a long skew culvert which will require more complex head and end walls. However, it is sometimes more economical to place the culvert perpendicular to the highway with certain acceptable changes in the channel alignment (see Linsley and Franzini, 1979).

(b) Culvert entrance structures

Properly designed entrance structures prevent bank erosion and improve the hydraulic characteristics of the culvert. The various types of entrance structures (end walls and wing walls) recommended are shown in Fig. 10.7.

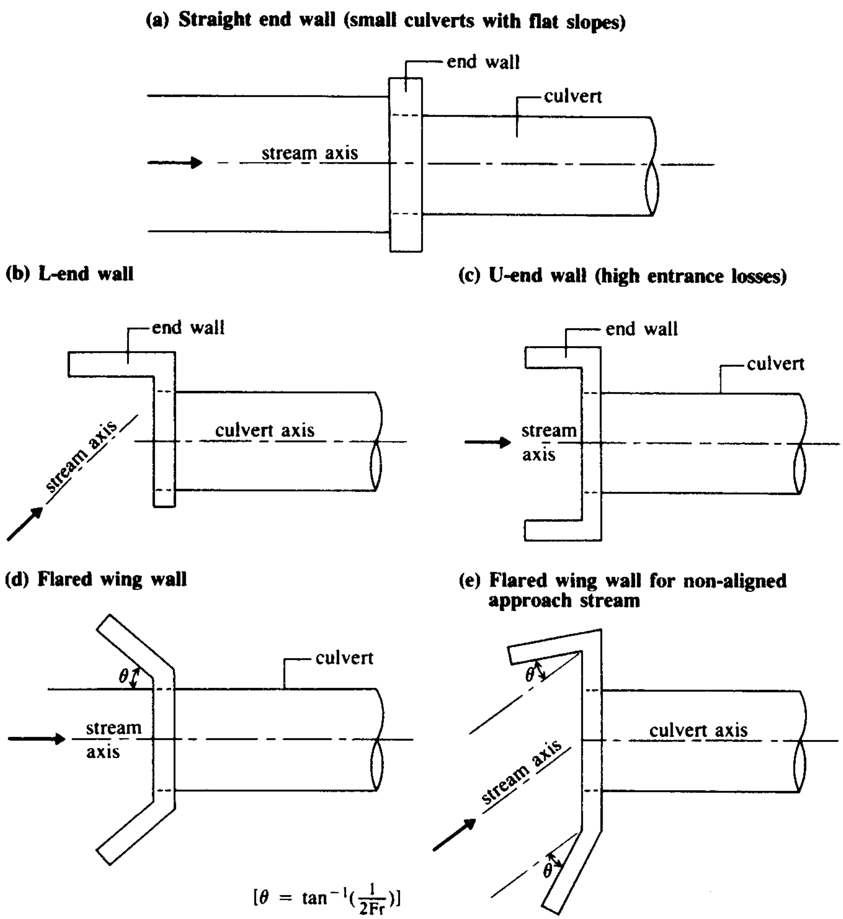

Fig. 10.7 Culvert entrance structures; plan views

A debris barrier (trash rack) must also be provided upstream of the culvert entrance to prevent the blockage of the barrel entrance.

In the case of a culvert with a submerged entrance, flaring the entrance will increase its capacity under a lower head for a given discharge. Such an arrangement for a box culvert (square or rectangular concrete barrel), the entrance area being double the barrel area over a length of $1.2D$, where D is the height of the barrel, is shown in Fig. 10.8.

A drop inlet structure with a necessary debris barrier (timber or concrete cribs) has to be provided whenever the culvert entrance is at the bed level (highway drainage facilities) of the drainage, requiring an abrupt break in the channel slope. Various arrangements of drop inlet culverts are shown in Fig. 10.9. The culvert sill length must be sufficient to discharge the design flow with a reasonably low-head water level. For high discharges, the entrance may be flared so as to increase the crest length. A flared entrance with a back wall (to prevent vortex action) considerably increases the inlet capacity. De-aeration chambers may have to be provided if a jump forms in the barrel of the culvert.

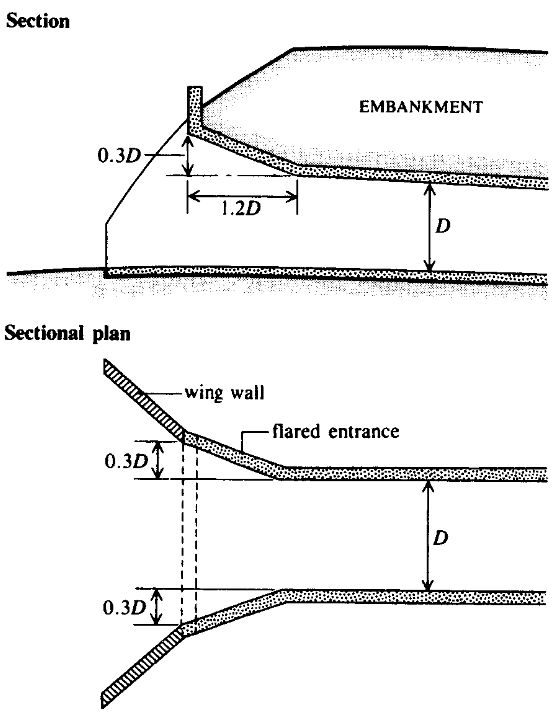

Fig. 10.8 Box culvert with flared entrance

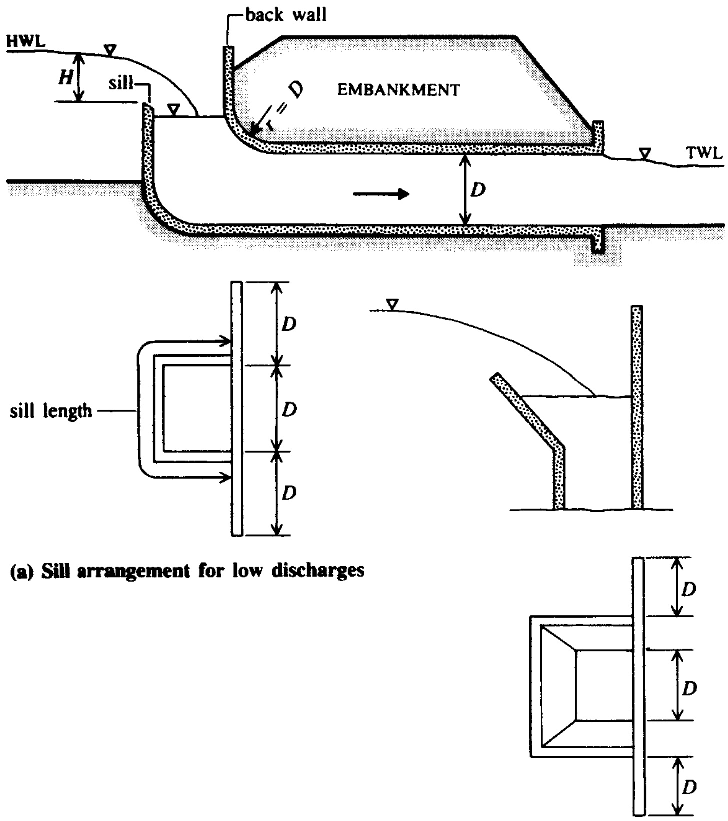

(a) Sill arrangement for low discharges

(b) Increased sill length with flared entry for high discharges

Fig. 10.9 Drop inlet culvert

(c) Culvert outlet structures

A proper device has to be provided at the outlet of a culvert to prevent the downstream erosion of the bed and the slopes of the embankment. For small discharges a straight or U-shaped end wall is sufficient. For moderate flows a flaring wing-walled outlet connecting the much wider downstream channel will reduce the scouring of the embankment and channel banks. The suggested flare angle for supercritical flows should be under 1 in 2, decreasing linearly with the flow Froude number. For subcritical flows it may be larger than 1 in 2.

(d) Scour below culvert outlets

The flow through a culvert may cause undesirable erosion (scour) at its unprotected outlet which can lead to undermining of the culvert structure.

Several researchers performed model tests on scour downstream of culvert structures and the combined results suggest the following design guidelines (see Breusers and Raudkivi, 1991):

$$\text{scour depth below bed level,} \quad y_s = 0.65D(U_o/U_{*c})^{1/3} \tag{10.1}$$

where U_o = flow velocity at exit and U_{*c} = Shields critical shear velocity $(=(\tau_c/\rho)^{1/2})$;

$$\text{scour width,} \quad B_s = 7.5DF_r^{2/3}, \tag{10.2}$$

$$\text{scour length,} \quad L_s = 15DF_r^{2/3} \tag{10.3}$$

where D = culvert height, $F_r = U_0/(gD)^{1/2}$, $0.27 < F_r < 2.7$ and $0.22 < d$ (mm) < 7.3. Equation (10.1) may be modified in the case of graded material as

$$y_s = 3.18DF_r^{0.57}\left(\frac{d_{50}}{D}\right)^{0.114}\sigma_g^{-0.4} \tag{10.4}$$

where $\sigma_g = (d_{84}/d_{16})^{1/2}$. In order to protect the channel bed against scouring, a minimum stone size is recommended as

$$d_s = 0.25DF_r \tag{10.5}$$

for low tail water levels. For high tail water levels ($>D/2$) the recommended stone size is reduced by $0.15D$.

Fletcher and Grace (1974) recommended a lining of trapezoidal cross-section downstream of the culvert exit extending to a length $= 5D$ with a bed slope of 1 in 10 followed by a curtain wall to a length $= D$ at a slope of 1 in 2; the side slopes of the trapezoidal lining are recommended to be 1 in 2. Alternatively, the design curves of Simons and Stevens (1972) may be used for non-scouring and scouring bed protection in rock basins (see Breusers and Raudkivi, 1991).

Blaisdell and Anderson (1988a, b) made a comprehensive study of scour at cantilevered pipe outlets and suggested the ultimate maximum scour hole depth, Z_{max}, below tailwater level (zero elevation) as

$$\frac{Z_{max}}{D} = -7.5[1 - e^{-0.6(F_{rd}-2)}] \tag{10.6}$$

for $Z_p/D \leq 1$ and

$$\frac{Z_{max}}{D} = -10.5[1 - e^{-0.35(F_{rd}-2)}] \tag{10.7}$$

for $Z_p/D > 1$ where D = pipe diameter, Z_p = height of pipe outlet above tailwater level and $F_{rd} = V/(g\Delta d_{50})^{1/2}$, V being the jet plunge velocity at the tailwater

$$(F_{rd} > 2; \ -2 < Z_p(\mathrm{m}) < 8; \text{ outlet slope, } 0 - 0.782).$$

The usual energy-dissipating devices (sloping apron, cistern, stilling basin, plunge pool, etc.) may have to be provided if the culvert discharge velocities are very high (Chapter 5).

10.2.3 Bridges

The presence of a bridge across a stream creates constricted flow through its openings because of (a) the reduction in the width of the stream due to piers and their associated end contractions and (b) the fluming of the stream itself (in the case of wide streams with flood plains) to reduce the costs of the structure.

Apart from (local) scour around the piers and bridge abutments and possible bed erosion, there is a considerable backwater effect of the bridge. The corresponding afflux (rise in upstream water level) depends on the type of flow (subcritical or supercritical). As most bridges are designed for subcritical flow conditions in order to minimize scour and choking problems, further discussions here are mainly confined to subcritical flow.

The establishment of afflux levels is extremely important for the design of upstream dykes and other protective works and also for the location of safe bridge deck levels (to avoid the flooding of the deck and any consequent structural damage). It is equally important to determine the minimum clear length of span (economic considerations) which will not cause undesirable afflux levels. In order to establish permissible upstream stage levels, detailed investigations of the properties along the stream have to be investigated. Downstream of the bridge the water levels are only influenced by the nearest control section below the bridge. These levels can therefore be established by backwater computation (for further information see Hamill, 1999).

(a) Backwater levels

SHORT CONTRACTIONS

In flow through a relatively short contracted section (narrow bridge without approach fluming) with only a few piers, the backwater problem may be relatively less important. Referring to Fig. 10.10, the change in

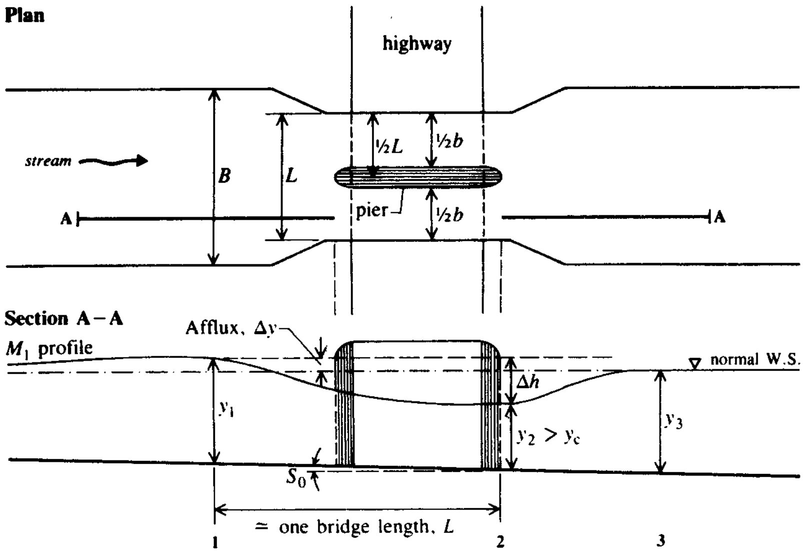

Fig. 10.10 Flow profile through bridge with contracted channel of relatively short length (subcritical flow)

water level, Δh, can be obtained by the energy equation between sections 1 and 2 (Kindsvater, Carter and Tracy, 1953) as

$$\Delta h = K_B V_2^2/2g + S_0 L/\sigma - \alpha_1 V_1^2/2g \tag{10.8}$$

where K_B is the bridge loss coefficient (Table 10.2), expressed as a function of the conveyance ratio,

$$\sigma = k_b/k_B, \tag{10.9}$$

Table 10.2 Bridge loss coefficient, K_B

σ	K_B
1.0	1.00
0.8	1.36
0.6	1.67
0.4	1.88
0.2	1.92

k_b being the conveyance of the gross contracted section with the same normal depth and roughness characteristics as the upstream approach section whose conveyance is k_B.

For rectangular unflumed sections the conveyance ratio (contraction ratio, $\alpha = 1 - \sigma$) becomes b/B, b being the clear width of the stream (of normal width, B) under the bridge (Fig. 10.10).

The bridge loss coefficient is also a function of the geometry of the bridge, its skew and eccentricity, and the submergence of the superstructure (i.e. the deck).

V_2 is the velocity just downstream of the piers, using the gross area under the bridge with the same upstream normal depth, and α_1 is the energy correction coefficient of the approach section. L is assumed to be equal to the bridge length (abutment to abutment), and S_0 is the normal bedslope of the unobstructed steam.

LONG CONTRACTIONS

In the case where the bridge has a number of large piers and/or long approach embankments contracting the water width, the backwater effect is considerable. Referring to the flow profile shown in Fig. 10.10, through such a long contracting section, Δy is the afflux entirely created by the presence of piers and channel contraction.

Momentum and continuity equations between sections 1 and 3 (assuming hydrostatic pressure distribution with a negligible bed slope and frictional resistance) result in

$$\Delta y/y_3 \simeq \{A + [A^2 + 12C_D(b/B)Fr_3^2]^{1/2}\}/6 \tag{10.10}$$

where

$$A = \{C_D(b/B) + 2\}Fr_3^2 - 2 \tag{10.11}$$

Fr_3 being the Froude number $(= V_3/(gy_3)^{1/2})$ at section 3.

Equation (10.10) should give good results if the drag coefficient C_D can be accurately estimated. The pier drag coefficient has been found to be a function of the velocity gradient of the approach flow, b/B, and the pier shape; however, owing to the non-availability of reliable drag coefficient values, the use of equation (10.10) is limited.

Yarnell's (1934) experimental data on the flow through bridge piers resulted in the following empirical equation:

$$\Delta y/y_3 = KFr_3^2(K + 5Fr_3^2 - 0.6)(\alpha + 15\alpha^4) \tag{10.12}$$

where

$$\alpha = 1 - \sigma = 1 - b/B \tag{10.13}$$

and K is a function of the pier shape according to Table 10.3.

Table 10.3 Values of *K* as a function of pier shape

Pier shape	*K*	*Remarks*
Semicircular nose and tail	0.9	All values applicable for piers with length to breadth ratio equal to 4; conservative estimates of Δy have been found for larger ratios;
Lens-shaped nose and tail	0.9	
Twin-cylinder piers with connecting diaphragm	0.95	
Twin-cylinder piers without diaphragm	1.05	Lens-shaped nose is formed from two circular curves, each of radius to twice the pier width and each tangential to a pier face
90° triangular nose and tail	1.05	
Square nose and tail	1.25	

Equation (10.12) is valid only if σ is large, i.e. the contraction cannot set up critical flow conditions between piers and choke the flow. If the flow becomes choked by excessive contraction the afflux increases substantially (Fig. 10.11). Referring to Fig. 10.11, the limiting values of σ (assuming uniform velocity at section 2) for critical flow at section 2 can be written as

$$\sigma = (2 + 1/\sigma)^3 Fr_3^4/(1 + 2Fr_3^2)^3. \tag{10.14}$$

In the case of choked flow the energy loss between sections 1 and 2 was given by Yarnell as

$$E_1 - E_2 = C_L V_1^2/2g \tag{10.15}$$

where C_L is a function of the pier shape (equal to 0.35 for square-edged piers and 0.18 for rounded ends, for a pier length:width ratio of 4). From equation (10.15) the upstream depth, y_1, can be calculated, from which the afflux Δy is obtained as $y_1 - y_3$.

Skewed bridges produce greater affluxes, and Yarnell found that a 10° skew bridge gave no appreciable changes, whereas a 20° skew produced about 250% more afflux values.

For backwater computations of arch bridges Martín-Vide and Prió (2005) recommend a head loss coefficient K for the sum of contraction and

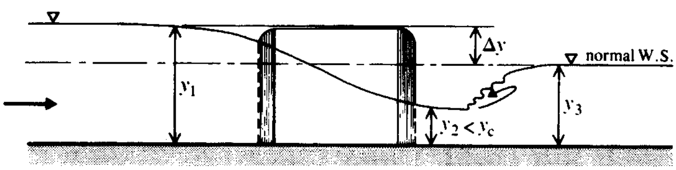

Fig. 10.11 Flow profile with choked flow conditions

expansion losses as $K = 2.3m - 0.345$, where m is the ratio of the obstructed and channel areas for $0.324 < m < 0.65$.

(b) Discharge computations at bridge piers

1. Nagler (1918) proposed a discharge formula for subcritical and near-critical flows as follows:

$$Q = K_N b(2g)^{1/2}(y_3 - \theta V_3^2/2g)(h_3 + \beta V_1^2/2g)^{1/2} \qquad (10.16)$$

the notation used in equation (10.16) being shown in Fig. 10.12(a). K_N is a coefficient depending on the degree of channel contraction and on the characteristics of the obstruction (Table 10.4); θ is a correction factor intended to reduce the depth y_3 to y_2 and β is the correction for the velocity of approach, depending on the conveyance ratio (Fig. 10.12(b)).

2. d'Aubuisson (1940) suggested the formula

$$Q = K_A b_2 y_3 (2gh_3 + V_1^2)^{1/2} \qquad (10.17)$$

where K_A is a function of the degree of channel contraction and of the shape and orientation of the obstruction (Table 10.4).

d'Aubuisson made no distinction between y_3 and y_2, and, although in many cases there is a small difference between them, equation (10.17) is recognized as an approximate formula.

3. Chow (1983) presents a comprehensive discussion of the discharge relationship between the flow through contracted openings and their shape, and other characteristics, together with a series of design charts produced by Kindsvater, Carter and Tracy (1953).

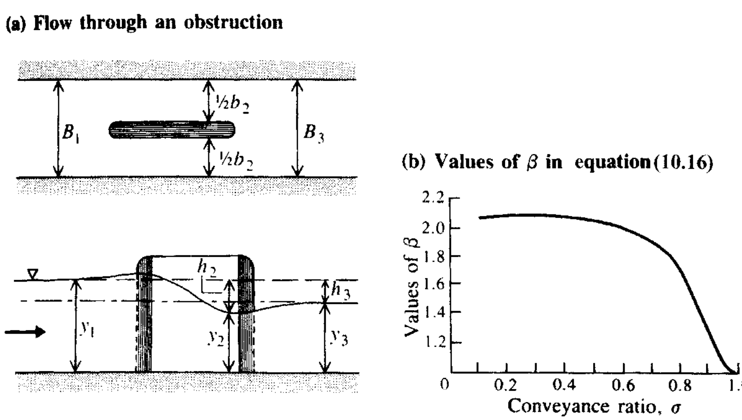

Fig. 10.12 Discharge computations through obstructions (definition sketch)

Table 10.4 Values of K_N and K_A

Type of pier	*Conveyance ratio, σ*									
	0.9		*0.8*		*0.7*		*0.6*		*0.5*	
	K_N	K_A	K_N	K_A	K_N	K_A	K_N	K_A	K_N	K_A
Square nose and tails	0.91	0.96	0.87	1.02	0.86	1.02	0.87	1.00	0.89	0.97
Semicircular nose and tails	0.94	0.99	0.92	1.13	0.95	1.20	1.03	1.26	1.11	1.31
90° triangular nose and tails	0.95		0.94		0.92					
Twin-cylinder piers with or without diaphragms	0.91		0.89		0.88					
Lens-shaped nose and tails	0.95	1.00	0.94	1.14	0.97	1.22				

(c) Scour depth under the bridge

If the contracted width (i.e. the bridge length, L) is less than the régime width, W (equation (9.9)), the normal scour depth, D_N, under the bridge is given by

$$D_N = R_s(W/L)^{0.61} \tag{10.18}$$

where R_s is the régime scour depth (equation (9.10)).

The maximum scour depth in a single-span bridge (no piers) with a straight approach (case 1) is about 25% more than the normal scour given by equation (10.18), whereas in the case of a multispan structure with a curved approach reach (case 2) it is 100% more than the normal scour. If the constriction is predominant, the maximum scour depth is the maximum of case 1 or case 2, or the value given by

$$D_{max} = R_s(W/L)^{1.56}. \tag{10.19}$$

(d) Scour around bridge piers

Several formulae based on experimental results have been proposed to predict the 'maximum' or 'equilibrium' scour depth (y_s, below general bed level) around bridge piers. In general, these assume the relationship

$$y_s/b' = \phi(y_0/b', Fr, d/b') \tag{10.20}$$

where b' is the pier width, y_0 is the upstream flow depth, d is the sediment size, and Fr is the flow Froude number.

Laursen's (1962) experimental results underestimate the scour depths, compared to many Indian experiments (Inglis, 1949) which suggest the formula (approach flow is normal to the bridge piers)

$$y_s/b' = 4.2(y_0/b')^{0.78}Fr^{0.52}. \tag{10.21}$$

The Indian field data also suggest that the scour depth should be taken as twice the régime scour depth.

In the case of live beds (a stream with bedload transport) the formula

$$y_s/y_0 = (B/b')^{5/7} - 1 \tag{10.22}$$

predicts the maximum equilibrium scour depth.

In a relatively deep flow a first-order estimate of (clear) local scour (around pier) may be obtained by

$$y_s = 2.3K_\alpha b' \tag{10.23}$$

where K_α = angularity coefficient which is a function of the pier alignment, i.e. angle of attack of approach flow.

Once again the best estimate will be achieved with the appropriate coefficients for flow depth, alignment, etc. (see Breusers and Raudkivi (1991) for further information). The live bed, however, contributes to an appreciably reduced local scour depth. If the sediment bed is distinctly layered and the covering layer (normally coarse material) is of a thickness less than the local scour depth the overall scouring phenomenon is quite different (see Ettema, 1980).

The flow penetrates the covering layer, triggering its disintegration. The disintegration of the covering layer may at times take place only in the downstream direction, leaving a stepped scour just upstream of the pier followed by a further local pier scour at its bottom. The stepped scour depth in the covering layer, H, is given by

$$H = \eta(y_2 - y_1) \tag{10.24}$$

where y_1 and y_2 are the uniform flow depths over a flat bed of grain roughness corresponding to the upstream surface particles (d_1) and the underlying surface fine particles (d_2) respectively; the coefficient for non-ripple-forming sediments $\eta = 2.6$ for design purposes. The total scour depth may lead to a gross underestimate if the lower layer is of very fine material (which may go into suspension).

The whole field of scour at bridge piers, piles and abutments is the subject of ongoing research focussing particularly on large scale experiments and development of scour with time. To proceed further with this topic is beyond the scope of this book and the reader is referred to e.g.

Breusers, Nicollet and Shen (1977), Clark and Novak (1983), Richardson and Richardson (1994), Melville and Chiu (1999), Melville and Coleman (2000), Oliveto and Hager (2002), Coleman, Lauchlan and Melville (2003), Sheppard, Odeh and Glasser (2004) and Dey and Barbhuiya (2005).

(e) Scour protection works around bridge piers

Although the presence of scour tends to reduce the backwater levels upstream of the bridge, the damage to the foundations of the structure may far outweigh the possible benefit. Hence protective measures, both to minimize the scour and to prevent undermining of the foundations, have to be taken. Piers with base diaphragms (horizontal rings) and multiple cylinder type piers have been found to minimize the scour considerably. The normal practice for protection of the foundation is to provide thick protective layers of stone or concrete aprons around the piers.

A riprap protection (Bonasoundas, 1973) in the shape of a longitudinal section of an egg with its broader end facing the flow is recommended for a cylindrical pier. The recommended overall width is $6b'$ and length $7b'$ of which $2.5b'$ is upstream of the pier. The thickness of riprap is $1/3b'$ with a maximum stone size, d, given by

$$d = 0.06 - 0.033U + 0.04U^2 \tag{10.25}$$

with U in metres per second and d in metres.

The mean critical flow velocity U_c (m s^{-1}) with a flow depth y_0 (m) is given by

$$U_c \approx 6d^{1/3}y_0^{1/6} \tag{10.26}$$

d being the armour stone size in metres (with $\rho_s = 2600\,\mathrm{kg\,m^{-3}}$).

For horizontal beds (US Army Coastal Engineering Research Center (1984); Chapter 14) the simplified empirical relationship is

$$U_c \approx 4.92d^{1/2}. \tag{10.27}$$

The riprap should be placed on a suitable inverted filter or a geotextile fabric (Fig. 9.11).

For further discussion of scour protection works refer to Zarrati *et al.* (2006) and Unger and Hager (2006). For a comprehensive treatment of bridge hydraulics (including hydraulic aspects of bridge construction and maintenance) refer to Neill (2004).

10.2.4 Dips

The dip is a shallow structure without excessive approach gradients. In arid regions, streams with infrequent flash floods and shallow depths (<0.3 m) may be allowed to flow through the dipped area. The upstream road edge should not be discontinuous with the stream bed in order to avoid scour, and at the downstream edge protection works such as a cut-off wall, concrete, or riprap paving must be provided. Also, the profile of the dip should, as far as possible, conform to the profile of the stream to minimize local disturbances to the flow.

The road surface has to withstand the expected flow velocities and debris. Bitumen-bound macadam may withstand velocities of up to $6\,\mathrm{m\,s^{-1}}$, whereas up to $7\,\mathrm{m\,s^{-1}}$ may be permitted on asphalted road surfaces. Low-level embankments, where occasional overtopping is permitted, must be protected against scour and bank-slope stability. The permissible mean velocities for a range of protective materials are suggested in Table 10.5 (Watkins and Fiddes, 1984).

The overflow discharge over an embankment may be predicted by using the weir formula of the type

$$Q = CbH^{3/2} \tag{9.29}$$

where C is the sill coefficient ($\mathrm{m^{1/2}\,s^{-1}}$), b is the length of the flow section and H is the total head upstream of the sill.

The coefficient C is a function of h/L (h is the head over a sill of width L) for free flow conditions. For non-modular flow conditions a correction factor, f, as a function of $h_{\mathrm{d/s}}/H$, may be incorporated in equation (9.29) (Tables 10.6 and 10.7).

Table 10.5 Permissible velocities to withstand erosion

Type of protection	*Velocity ($\mathrm{m\,s^{-1}}$)*
Grass turfing:	
Bermuda grass	$\simeq$2.0
buffalo grass	1.5
Cobbles:	
$\simeq$100 mm	3.5
$\simeq$40 mm	2.5
Coarse gravel and cobbles ($\simeq$25 mm)	2.0
Gravel ($\simeq$10 mm)	1.5

Table 10.6 Range of values of *C* for free flow over the embankment

Type of surface	*Range of h/L*	*Range of C*
Paved surface	0.15	1.68
	0.20	1.69
	>0.25	1.70
Gravel surface	0.15	1.63
	0.20	1.66
	0.25	1.69
	0.30	1.70

Table 10.7 Correction factor, *f* (non-modular flows)

Type of surface	*Range of* $h_{d/s}/H$	*f*
Paved surface	≤0.8	1.0
	0.9	0.93
	0.95	0.8
	0.99	0.5
Gravel surface	≤0.75	1.0
	0.8	0.98
	0.9	0.88
	0.95	0.68
	0.98	0.50

Worked Example 10.3

Establish the stage (headwater level)–discharge relationship for a concrete rectangular box culvert, using the following data: width = 1.2 m; height = 0.6 m; length = 30 m; slope = 1 in 1000; Manning's $n = 0.013$; square-edged entrance conditions; free jet outlet flow; range of head water level for investigation = 0–3 m; neglect the velocity of approach.

Solution

1. $H/D \leq 1.2$. For $H < 0.6$ m, free flow open-channel conditions prevail. Referring to Fig. 10.6 and assuming that a steep slope entry gives entrance control, i.e. the depth at the inlet is critical, for $H = 0.2$ m, ignoring entry loss $y_c = (2/3) \times 0.2 = 0.133$ m and $V_c = 1.142\,\text{m s}^{-1}$. This gives the critical slope $(Vn)^2/R^{4/3} = 0.00424$. Therefore the slope of the culvert is mild and hence subcritical flow analysis gives the following results:

$$Q = 1.2y_0[1.2y_0/(1.2 + 2y_0)]^{2/3}\,(0.001)^{1/2}/0.013$$

$$= 2.92y_0[1.2y_0/(1.2 + 2y_0)]^{2/3}; \qquad \text{(i)}$$

y_0 (m)	Q ($m^3 s^{-1}$)(equation (i))	y_c (m)
0.2	0.165	0.124
0.4	0.451	0.243
0.6 (=D)	0.785	0.352

At the inlet over a short reach,

$$H = y_0 + V^2/2g + K_e V^2/2g. \tag{ii}$$

The entrance loss coefficient, K_e, is as follows:

for a square-edged entry, 0.5;

for a flared entry, 0.25;

for a rounded entry, 0.05;

y_0 (m)	H (m) (equation (ii))	Q ($m^3 s^{-1}$)
0.2	0.236	0.165
0.4	0.467	0.451
0.6	0.691	0.785
orifice $\leftarrow > 0.6 \leftarrow (1.2D =)$	0.72 $\longrightarrow$	0.817 (by interpolation)

2. $H/D \geq 1.2$.
   (a) For orifice flow

$$Q = C_d(1.2 \times 0.6)[2g(H - D/2)]^{1/2}. \tag{iii}$$

With $C_d = 0.62$ the following results are obtained:

H(m)	Q ($m^3 s^{-1}$)	y_0 (m) (equation (i))
0.72	1.29	$>0.6 \rightarrow$ no orifice flow exists

(b) For pipe flow the energy equation gives

$$H + S_0 L = D + h_L$$

where

$$h_L = K_e V^2/2g + (Vn)^2 L/R^{4/3} + V^2/2g.$$

Thus

$$Q = 2.08(H - 0.57)^{1/2}. \tag{iv}$$

	H (m)	*Q ($m^3 s^{-1}$) (equation (iv))*
$y_0 \simeq 0.6$ (equation (i) ←	0.691	0.723
	0.72	0.805
	1.00	1.364
	2.00	2.487
	3.00	3.242

During rising stages the barrel flows full from $H = 0.72$ m and during falling stages the flow becomes free-surface flow when $H = 0.691$ m.

The following table summarizes the results:

H (m)	*Q ($m^3 s^{-1}$)*	*Type of flow*
Rising stages		
0.236	0.165	Open channel
0.467	0.451	Open channel
0.691	0.785	Open channel
0.720	0.805	Pipe flow
1.00	1.364	Pipe flow
2.00	2.487	Pipe flow
3.00	3.242	Pipe flow
Falling stages		
2.00	2.487	Pipe flow
1.00	1.364	Pipe flow
0.72	0.805	Pipe flow
0.691	0.723	Pipe flow
0.691	0.785	Open channel
0.467	0.451	Open channel
0.236	0.165	Open channel

Worked Example 10.4

Examine the stage–discharge relationship for the culvert in Worked example 10.3 if the bedslope is 1 in 100.

Solution

Rising stages are as follows.

1. For the open channel, preliminary calculations now indicate that the slope is steep and hence the entrance is the control, with the critical depth at the entry. The energy equation at the inlet gives

$$H = 1.5V^2/2g + y = 1.75y_c. \qquad \text{(v)}$$

y_c (m)	H (m)	Type	Q ($m^3 s^{-1}$)
0.2	0.35	Free	0.336
0.4	0.70	Free	0.951
0.6	1.50 (>1.2D)	Submerged	–
0.411	0.72 (=1.2D)	Just free	0.990

2. For the orifice (equation (iii)),

H (m)	Type	Q ($m^3 s^{-1}$)	y_0 (m) (equation (i) with $S_0 = 1/100$)*
0.72	Orifice	1.29	0.36
1.00	Orifice	1.66	0.44
2.00	Orifice?	2.58	0.61 (>D)
1.95	Orifice	2.54	0.60

*$Q = 9.23y_0[1.2y_0/(1.2 + 2y_0)]^{2/3}$

3. For pipe flow (equation (iv) changes):

$$Q = 2.08(H - 0.3)^{1/2} \text{ for } S_0 = 1/100.$$

H (m)	Type	Q ($m^3 s^{-1}$)	y_0 (m) (equation (i))
1.95	Pipe flow	2.67	
2.00	Pipe flow	2.71	
3.00	Pipe flow	3.42	
Falling stages			
3.00	Pipe flow	3.42	
2.00	Pipe flow	2.71	
1.95	Pipe flow	2.67	
1.74	← Pipe flow	← 2.50	← 0.60
1.74 →	Orifice →	2.37	
1.00	Orifice	1.66	
0.72	Orifice	1.29	
0.72	Just free	0.99	
0.70	Free	0.951	
0.35	Free	0.336	

Worked Example 10.5

The design flood with a 20-year return period is $15\,m^3 s^{-1}$. Design the culvert-type cross-drainage structure with a high embankment with the following data: culvert length = 30 m; slope = 1.5%; available pipe barrel, corrugated pipes in multiples of 250 mm diameter; Manning's $n = 0.024$. The barrel protrudes from the embankment with no end walls, with an entry loss coefficient of 0.9. The maximum permissible head water level is 4 m above the invert with the barrel flowing full.

Solution

For full pipe flow the energy equation gives

$$H + 30 \times 0.015 = D + 0.9V^2/2g + (Vn)^2 L/R^{4/3} + V^2/2g. \tag{vi}$$

Equation (vi) gives the following results:

D (m)	*H (m)*
1.500	12.61
2.000	4.74
2.500	3.25
2.250	3.70

Therefore provide a 2.25 m diameter barrel for $H \leq 4.0$ m.

Check for the flow conditions:

$$H/D = 3.70/2.25 = 1.65 > 1.2.$$

Hence the inlet is submerged. Using Manning's equation with the maximum discharge, the required diameter for the flow to be just free is 2.32 m, which is greater than the diameter provided. Hence the barrel flows full (under pressure).

Note that an improved entrance would considerably reduce the head loss and allow a smaller-diameter barrel to discharge the flood flow. For example a flare-edged entry (loss coefficient = 0.25) would produce a head of 3.93 m (<4.0 m) with a barrel of 2.00 m diameter.

Worked Example 10.6

A road bridge of seven equal span lengths crosses a 106 m wide river. The piers are 2.5 m thick, each with semicircular noses and tails, and their length:breadth ratio is 4. The streamflow data are given as follows: discharge = 500 $m^3 s^{-1}$; depth of flow downstream of the bridge = 2.50 m. Determine the afflux upstream of the bridge.

Solution

The velocity at the downstream section, $V_3 = 500/106 \times 2.5 = 1.887\ m\,s^{-1}$. Therefore the Froude number, $Fr_3 = 0.381$. Flow conditions within the piers are as follows: the limiting value of $\sigma \simeq 0.55$ (equation (10.14)), while the value of σ provided = $b/B = 13/15.5 = 0.839$. Since the value of σ provided is more than the limiting σ value, subcritical flow conditions exist between the piers. Using equation (10.12) with $K = 0.9$ (Table 10.3) and $\alpha = 1 - \sigma = 0.161$, the afflux, $\Delta y = 5.41 \times 10^{-2}$ m.

10.3 Drop structures

10.3.1 Introduction

A drop (or fall) structure is a regulating structure which lowers the water level along its course. The slope of a canal is usually milder than the terrain slope as a result of which the canal in a cutting at its headworks will soon outstrip the ground surface. In order to avoid excessive infilling the bed level of the downstream canal is lowered, the two reaches being connected by a suitable drop structure (Fig. 10.13).

The drop is located so that the fillings and cuttings of the canal are equalized as much as possible. Wherever possible, the drop structure may also be combined with a regulator or a bridge. The location of an offtake from the canal also influences the fall site, with offtakes located upstream of the fall structure.

Canal drops may also be utilized for hydropower development, using bulb- or propeller-type turbines. Large numbers of small and medium-sized drops are desirable, especially where the existing power grids are far removed from the farms. Such a network of micro-installations is extremely helpful in pumping ground water, the operation of agricultural equipment, village industries, etc. However, the relative economy of providing a large number of small falls versus a small number of large falls must be considered. A small number of large falls may result in unbalanced earthwork but, on the other hand, some savings in the overall cost of the drop structures can be achieved.

Drops are usually provided with a low crest wall and are subdivided into the following types: (i) the vertical drop, (ii) the inclined drop and (iii) the piped drop.

The above classification covers only a part of the broad spectrum of drops, particularly if structures used in sewer design are included; a comprehensive survey of various types of drops has been provided, e.g. by Merlein, Kleinschroth and Valentin (2002); Hager (1999) includes the treatment of drop structures in his comprehensive coverage of wastewater structures and hydraulics.

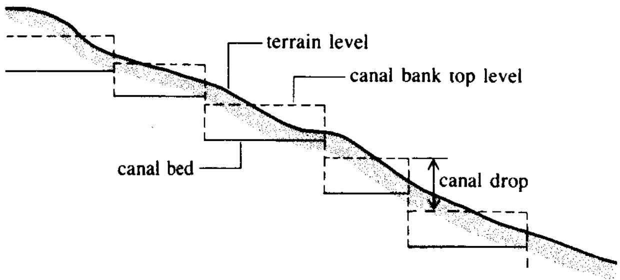

Fig. 10.13 Location of canal drops

10.3.2 Vertical drop structures

(a) Common (straight) drop

The common drop structure, in which the aerated free-falling nappe (modular flow) hits the downstream basin floor, and with turbulent circulation in the pool beneath the nappe contributing to energy dissipation, is shown in Fig. 10.14.

The following equations fix the geometry of the structure in a suitable form for steep slopes:

drop number, $D_r = q^2/g^{d3}$ (10.28)

where q is the discharge per metre width;

basin length, $L_B/d = 4.3D_r^{0.27} + L_j/d$; (10.29)

pool depth under nappe, $Y_P/d = D_r^{0.22}$; (10.30)

sequent depths, $y_1/d = 0.54D_r^{0.425}$; (10.31)

$y_2/d = 1.66D_r^{0.27}$; (10.32)

here d is the height of the drop crest above the basin floor and L_j the length of the jump.

A small upward step, h (around $0.5 < h/y_1 < 4$), at the end of the basin floor is desirable in order to localize the hydraulic jump formation. Forster and Skrinde (1950) developed design charts for the provision of such an abrupt rise.

The USBR (Kraatz and Mahajan, 1975) impact block type basin also provides good energy dissipation under low heads, and is suitable if the

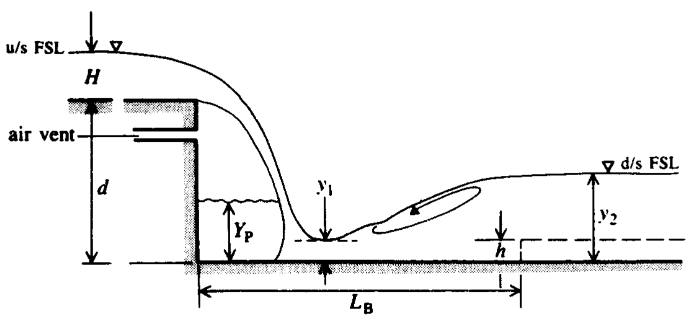

Fig. 10.14 Common drop structure (after Bos, 1976)

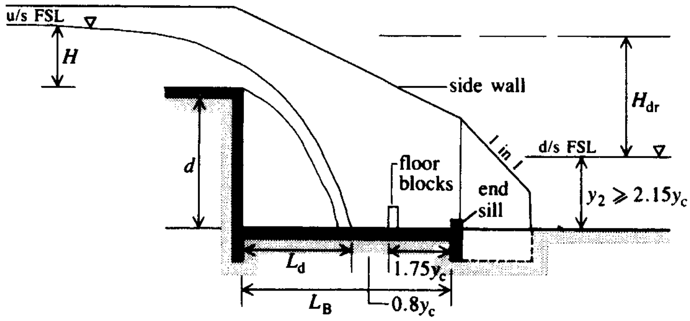

Fig. 10.15 Impact block type basin (after Bos, 1976)

tailwater level (TWL) is greater than the sequent depth, y_2. The following are the suggested dimensions of such a structure (Fig. 10.15):

basin length $L_B = L_d + 2.55y_c$; (10.33)

location of impact block, $L_d + 0.8y_c$; (10.34)

minimum TW depth, $y_2 \geq 2.15y_c$; (10.35)

impact block height, $0.8y_c$; (10.36)

width and spacing of impact block, $0.4y_c$; (10.37)

end sill height, $0.4y_c$; (10.38)

minimum side wall height, $y_2 + 0.85y_c$; (10.39)

here y_c is the critical depth.

The values of L_d can be obtained from Fig. 10.16.

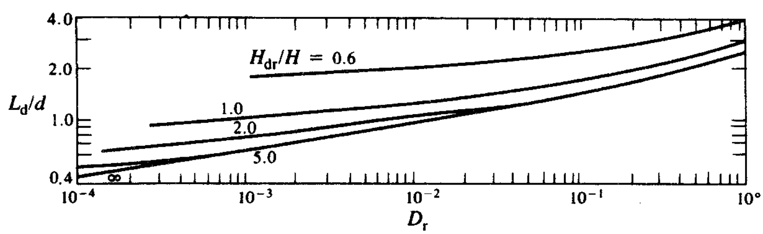

Fig. 10.16 Values of L_d/d (after Bos, 1976)

(b) Sarda-type fall (India)

This is a raised-crest fall with a vertical impact, consisting of a crest wall, upstream and downstream wing walls, an impervious floor and a cistern, and downstream bank and bed protection works (Fig. 10.17).

The crest design is carried out as follows. The crest length is normally kept equal to the bed width of the canal; however, an increase in length by an amount equal to the flow depth takes into account any future increase in discharge. Fluming may be provided to reduce the cost of construction of the fall. A flumed fall with a fluming ratio equal to $2F_1$, where F_1 is the approach flow Froude number, creates no choking upstream of the fall. A canal is not usually flumed beyond 50%. Whenever the canal is flumed, both upstream (contracting) and downstream (expanding) transitions have to be provided (Fig. 10.3).

The crest level must be so fixed that it does not create changes in upstream water levels (backwater or drawdown effects). If the reduced level (RL) of the full supply level (FSL) is Y, the RL of the total energy line (TEL) is

$$E = Y + V_a^2/2g \tag{10.40}$$

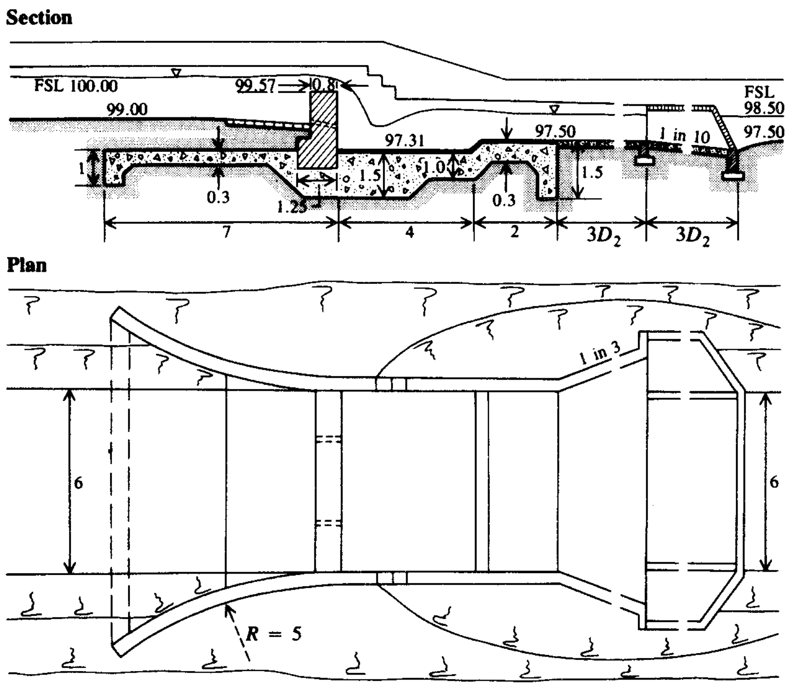

Fig. 10.17 Sarda fall layout (Worked example 10.7); dimensions in metres

where V_a is the approach velocity.

If L_e is the effective length of the crest, the head causing flow is given by the weir formula:

$$H = (Q/C_d L_e)^{2/3} \tag{10.41}$$

where Q is the discharge and C_d is the discharge coefficient of the crest. Therefore, the RL of the crest is $E - H$.

Two types of crest are used (Fig. 10.18); the rectangular one for discharges up to $10\,m^3 s^{-1}$ and the trapezoidal one for larger discharges (see Punmia and Lal, 1977).

The following are the design criteria established by extensive model studies at the Irrigation Research Institute in India.

1. For a rectangular crest,

$$\text{top width,}\quad B = 0.55 d^{1/2}\ \text{(m)}, \tag{10.42}$$

$$\text{base width,}\quad B_1 = (H + d)/S_s, \tag{10.43}$$

where S_s is the relative density of the crest material (for masonry, $S_s \simeq 2$). The discharge is given by the following formula:

$$Q = 1.835 L H^{3/2} (H/B)^{1/6}. \tag{10.44}$$

2. For a trapezoidal crest,

$$\text{top width,}\quad B = 0.55(H + d)^{1/2}\ \text{(m)}. \tag{10.45}$$

For the base width, B_1, upstream and downstream slopes of around 1

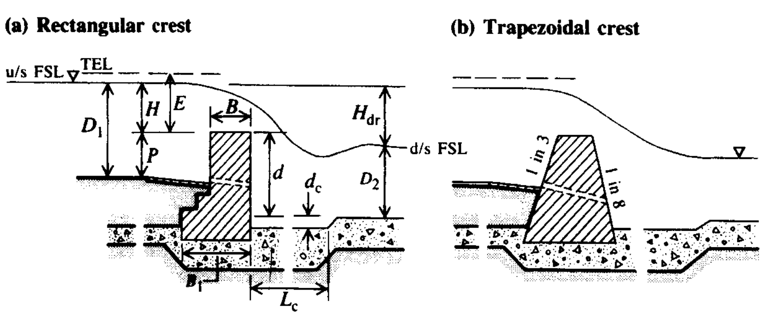

Fig. 10.18 Sarda fall crests

in 3 and 1 in 8 are usually recommended. The discharge is given by the following formula:

$$Q = 1.99LH^{3/2}(H/B)^{1/6}. \tag{10.46}$$

3. Design of cistern is as follows:

$$\text{length,} \quad L_c = 5(EH_{dr})^{1/2}; \tag{10.47}$$

$$\text{depth,} \quad d_c = \frac{1}{4}(EH_{dr})^{2/3}. \tag{10.48}$$

4. Minimum length of impervious floor downstream of the crest,

$$L_{bd} = 2(D_1 + 1.2) + H_{dr}. \tag{10.49}$$

(c) YMGT-type drop (Japan)

This type of drop is generally used in flumed sections suitable for small canals, field channels, etc., with discharges up to $1\,m^3 s^{-1}$ (Fig. 10.19). The following are the recommended design criteria:

1. sill height, P varies from 0.06 m to 0.14 m with the unit discharge q between 0.2 and $1.0\,m^3 s^{-1} m^{-1}$;
2. depth of cistern, $d_c = 1/2(E_c H_{dr})^{1/2}$; (10.50)
3. length of cistern, $L_c = 2.5L_d$, (10.51)

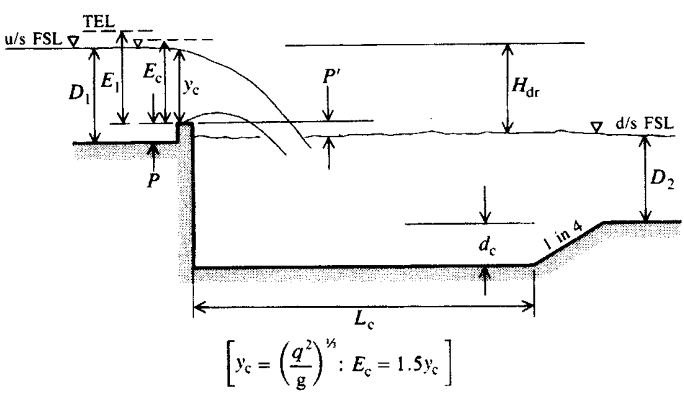

Fig. 10.19 YMGT-type drop, Japan (Kraatz and Mahajan, 1975)

where $L_d = L_{d1} + L_{d2}$ and

$$L_{d1}/E_c = 1.155[(P'/E_c) + 0.33]^{1/2}, \tag{10.52}$$

$$L_{d2} = (D_2 + d_c)\cot\alpha, \tag{10.53}$$

$$\cot\alpha = y_c/L_{d1}. \tag{10.54}$$

Alternatively, the recommendations of the IRI, India (previous section) may also be adopted.

(d) Rectangular weir drop with raised crest (France)

SOGREAH (Kraatz and Mahajan, 1975) have developed a simple structure suitable for vertical drops of up to 7 m (for channel bed widths of 0.2–1 m with flow depths (at FSL) of 0.1–0.7 m): Fig. 10.20 shows its design details.

1. For the design of crest,

$$\text{discharge,} \quad Q = CL(2g)^{1/2}H^{3/2}, \tag{9.29}$$

where $C = 0.36$ for the vertical upstream face of the crest wall and 0.40 for the rounded upstream face (5–10 cm radius). The crest length, $L = L_B - 0.10$ m for a trapezoidal channel and is B_1 (the bed width) for rectangular channels.

2. For the design of cistern,

$$\text{volume of basin,} \quad V = QH_{dr}/150\ (\text{m}^3), \tag{10.55}$$

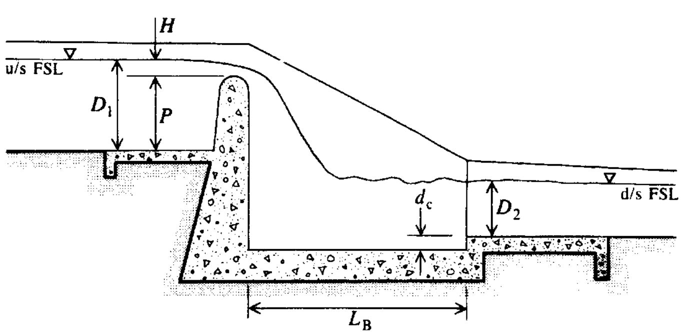

Fig. 10.20 Rectangular weir drop with raised crest, France (Kraatz and Mahajan, 1975)

$$\text{width of basin,} \quad W_B = V/[L_B(D_2 + d_c)], \tag{10.56}$$

where the depth of the basin, $d_c \simeq 0.1$–0.3 m.

10.3.3 Inclined drops or chutes

(a) Common chute

This type of drop has a sloping downstream face (between 1/4 and 1/6, called a glacis) followed by any conventional type of low-head stilling basin; e.g. SAF or USBR type III (Chapter 5). The schematic description of a glacis-type fall with a USBR type III stilling basin, recommended for a wide range of discharges and drop heights, is shown in Fig. 10.21.

(b) Rapid fall type inclined drop (India)

This type of fall is cheap in areas where stone is easily available, and is used for small discharges of up to $0.75\,m^3 s^{-1}$ with falls of up to 1.5 m. It consists of a glacis sloping between 1 in 10 and 1 in 20. Such a long glacis assists in the formation of the hydrualic jump, and the gentle slope makes the uninterrupted navigation of small vessels (timber traffic, for example) possible.

(c) Stepped or cascade-type fall

This consists of stone-pitched floors between a series of weir blocks which act as check dams and are used in canals of small discharges; e.g. the tail of a main canal escape. A schematic diagram of this type of fall is shown in Fig. 10.22.

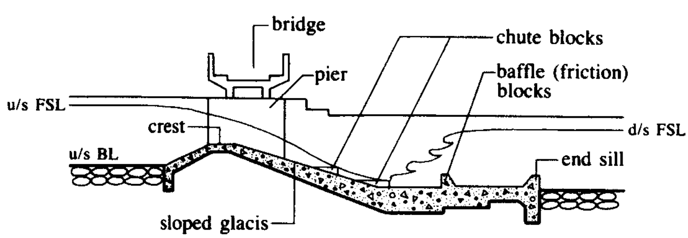

Fig. 10.21 Sloping glacis type fall with USBR type III stilling basin

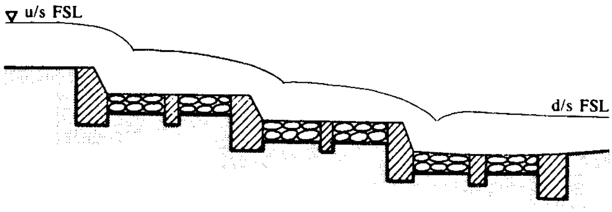

Fig. 10.22 Stepped or cascade-type fall

10.3.4 Piped drops

A piped drop is the most economical structure compared with an inclined drop for small discharges of up to $50\,l\,s^{-1}$. It is usually equipped with a check gate at its upstream end, and a screen (debris barrier) is installed to prevent the fouling of the entrance.

(a) Well drop structure

The well drop (Fig. 10.23) consists of a rectangular well and a pipeline followed by a downstream apron. Most of the energy is dissipated in the well, and this type of drop is suitable for low discharges (up to $50\,l\,s^{-1}$) and high drops (2–3 m), and is used in tail escapes of small channels.

(b) Pipe fall

This is an economical structure generally used in small channels. It consists of a pipeline (precast concrete) which may sometimes be inclined sharply downwards (USBR and USSR practice) to cope with large drops. However, an appropriate energy dissipator (e.g. a stilling basin with an end sill) must be provided at the downstream end of the pipeline.

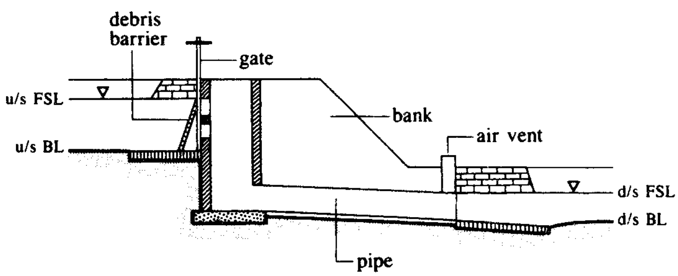

Fig. 10.23 Well drop structure

10.3.5 Farm drop structures

Farm channel drops are basically of the same type and function as those in distribution canals, the only differences being that they are smaller and their construction is simpler.

The notch fall type of farm drop structure (precast concrete or timber) consists of a (most commonly) trapezoidal notch in a crested wall across the canal, with the provision of appropriate energy-dissipation devices downstream of the fall. It can also be used as a discharge-measuring structure.

The details of a concrete check drop with a rectangular opening, widely used in the USA, are shown in Fig. 10.24. Up to discharges of about $0.5\,m^3\,s^{-1}$, the drop in the downstream floor level (C) is recommended to be around 0.2 m and the length of the apron (L) between 0.75 m and 1.8 m over a range of drop (D) values of 0.3–0.9 m.

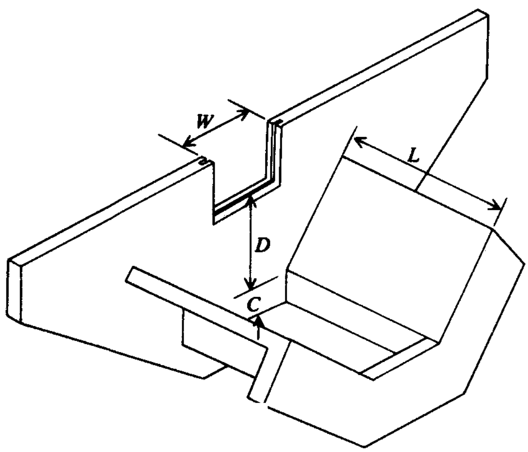

Fig. 10.24 Notch fall: concrete check drop (USA)

Worked Example 10.7

Design a Sarda-type fall using the following data: full supply discharge = $28\,m^3\,s^{-1}$; upstream FSL = 100.00 m AOD; downstream FSL = 98.50 m AOD; upstream bed level = 99.00 m AOD; downstream bed level = 97.50 m AOD; upstream bed width = 6.00 m; downstream bed width = 6.00 m; drop, H_{dr} = 1.50 m; safe exit gradient of the subsoil = 1 in 5.

Solution

CREST DESIGN

Adopt a rectangular crest (Fig. 10.18). $B = 0.55d^{1/2}$; for a trapezoidal crest, $B = 0.55\ (H + d)^{1/2}$ and $H + d = D_1 + 99.00 - 97.50 = 2.5$ m. Hence B (trapezoidal crest) = 0.87 m. Choose a rectangular crest, width $B = 0.80$ m. Adopting a crest length of $L = 6$ m, equation (10.51) gives the head over the crest,

$$H = 0.43\,\text{m}.$$

Check for B: the crest level = 100.00 − 0.43 = 99.57 m AOD. Therefore $d = 99.57 - 97.50 = 2.07$ m and $B = 0.55d = 0.79$ m. Therefore a crest width of 0.8 m is satisfactory.

The base width, $B_1 = 1.25$ m (equation (10.50) with $S_s = 2.0$). The velocity of approach (assuming a 1:1 trapezoidal channel) = 2.8/(6 + 1)1 = 0.4 m s^{-1}. Therefore the upstream total energy level (TEL) = 100.000 + 0.008 = 100.008 m AOD, and $E = 100.008 - 99.57 = 0.438$ m.

The depth of the cistern, $d_c = 0.19$ m (equation (10.55)), and the length of the cistern, $L_c \simeq 4$ m (equation (10.54)). The RL of the cistern bed = 97.50 − 0.19 = 97.31 m AOD.

IMPERVIOUS FLOOR DESIGN (WORKED EXAMPLE 9.1 PROVIDES DETAILED CALCULATIONS)

The maximum seepage head, $H_s = d$ (with no water downstream, and the upstream water level at crest level). Adopting nominal upstream and downstream cut-off depths of 1 m and 1.5 m respectively, the base length of the impervious floor for the exit gradient of 1 in 5 is approximately 13 m. The length of the impervious floor downstream of the crest is approximately 6 m (equation 10.56)). The upstream floor thickness (nominal thickness of 0.3 m) at the toe of the crest is approximately 1.5 m, and at 5 m from the toe it is approximately 0.14 m; adopt a minimum of 0.3 m.

Appropriate energy-dissipating devices (for large discharges) and upstream and downstream bed protection works must be provided. The detailed layout of the design is shown in Fig. 10.17.

References

d'Aubuisson, J.F. (1940) *Traité d'Hydraulique*, 2nd edn, Pitois, Levraut et Cie, Paris.

Blaisdell, F.W. and Anderson, CL. (1988a) A comprehensive generalized study of scour at cantilevered pipe outlets. *Journal of Hydraulic Research*, 26 (4): 357–76.

—— (1988b) A comprehensive study of scour of cantilevered pipe outlets. *Journal of Hydraulic Research*, 26 (5): 509–24.

Bonasoundas, M. (1973) *Strömungsvorgang und Kolkproblem*, Report 28, Oscar von Miller Institute, Technical University, Munich.

Bos, M.G. (ed.) (1976) *Discharge Measurement Structures*, Laboratorium voor Hydraulica en Afvoerhydrologia, Wageningen.

Breusers, H.N.C. and Raudkivi, A.J. (1991) *Scouring*, IAHR Hydraulic Structures Design Manual, Vol. 2, Balkema, Rotterdam.

Breusers, H.N.C., Nicollet, G. and Shen, H.W. (1977) Local scour around cylindrical piers. *Journal of Hydraulic Research*, 15 (3): 211–52.

Chanson, H. (1999) *Hydraulics of Open Channels – An Introduction*, Arnold, London.

Charbeneau, R.J., Henderson, A.D. and Sherman, L.C. (2006) Hydraulic performance curves for highway culverts, *J. of Hydraulic Engineering ASCE*, 132, No. 5: 474–81.

Chow, V.T. (1983) *Open Channel Hydraulics*, McGraw-Hill, New York.

Clark, A. and Novak, P. (1983) Local erosion at vertical piles by waves and currents, in *Proceedings of the IUTM Symposium on Seabed Mechanics*, Newcastle upon Tyne.

Coleman, S.E., Lauchlan, C.S. and Melville, B.W. (2003) Clear-water scour development at bridge abutments, *J. of Hydraulic Research*, IAHR, 41, No. 5: 521–31.

Dey, S. and Barbhuiya, A.K. (2005) Time variation of scour at abutments, *J. of Hydraulic Engineering*, ASCE, 13, No. 1: 11–23.

Ettema, R. (1980) *Scour at Bridge Piers*, Report 216, School of Civil Engineering, University of Auckland.

Fletcher, B.P. and Grace, J.L., Jr. (1974) *Practical Guidance for Design of Lined Channel Expansions at Culvert Outlets*, Technical Report H-74-9, US Army Engineers Waterways Experimental Station, Vicksburg.

Forster, J.W. and Skrinde, R.A. (1950) Control of the hydraulic jump by sills. *American Society of Civil Engineers Transactions*, 115: 973–87.

Hager, W.H. (1999) *Wastewater Hydraulics*, Springer Verlag, Berlin.

Hamill, L. (1999) *Bridge Hydraulics*, E & FN Spon, London.

Hinds, J. (1928) The hydraulic design of flume and siphon transitions. *Transactions of the American Society of Civil Engineers*, 92: 1423–59.

Inglis, C. (1949) *The Behaviour and Control of Rivers and Canals*, Research Publication 13, Central Water Power Irrigation and Navigation Report, Poona Research Station.

Kindsvater, C.E., Carter, R.W. and Tracy, H.J. (1953) *Computation of Peak Discharge at Contractions*, Circular 284, USGS.

Kraatz, D.B. and Mahajan, I.K. (1975) *Small Hydraulic Structures – Irrigation and Drainage*, FAO, Rome, Papers 26/1 and 26/2.

Laursen, E.M. (1962) Scour at bridge crossings. *Transactions of the American Society of Civil Engineers, Part 1*, 127: 166–209.

Linsley, R.K. and Franzini, J.B. (1979) *Water Resources Engineering*, 3rd edn, McGraw-Hill, New York.

Martín-Vide, J.P. and Prió, J.M. (2005) Backwater of arch bridges under free and submerged conditions, *J. of Hydraulic Research*, IAHR, 43, No. 5: 515–21.

Mays, L.W. (ed.) (1999) *Hydraulic Design Handbook*, McGraw-Hill, New York.

Melville, B.W. and Chiu, Yee-Meng (1999) Time scale for local scour at bridge piers, *J. of Hydraulic Engineering*, ASCE, 125, No. 1: 59–65.

Melville, B.W. and Coleman, S. (2000) *Bridge Scour*, Water Resources Publications, Colorado.

Merlein, J., Kleinschroth, A. and Valentine, F. (2002) *Systematisierung von Absturzbauwerken*, Mitteilung N. 69, Lehrstuhl und Laboratorium für Hydraulik und Gewässerkunde, Technische Universität, München.

Nagler, F.A. (1918) Obstruction of bridge piers to the flow of water. *Transactions of the American Society of Civil Engineers*, 82: 334–95.

Neil, C. (ed.) (2004) *Guide to Bridge Hydraulics*, 2nd edn, Thomas Telford, London, and Transportation Association of Canada, Ottawa.

Oliveto, G. and Hager, W.H. (2002) Temporal evolution of clear-water pier and abutment scour, *J. of Hydraulic Engineering*, ASCE, 128, No. 9: 811–20.

Punmia, B.C. and Lal, P.B.B. (1977) *Irrigation and Water Power Engineering*, 4th edn, Standard Publishers, New Delhi.

Ramsbottom, D., Day, R. and Rickard, C. (1997) *Culvert Design Manual*, CIRIA Report 168, Construction Industry Research and Information Association (CIRIA), London.

Ranga Raju, K.G. (1993) *Flow Through Open Channels*, 2nd edn, Tata McGraw-Hill, New Delhi.

Richardson, J.R. and Richardson, E.V. (1994) Practical method for scour prediction at bridge piers, in *Hydraulic Engineering '94* (eds J.V. Cotroneo and R.R. Rumer), *Proceedings of the ASCE Conference*, Buffalo, NY, 1994, American Society of Civil Engineers, New York.

Sheppard, D.M., Odeoh, M. and Glasser, T. (2004) Large scale clear-water local scour experiments, *J. of Hydraulic Engineering*, ASCE, 130, No. 10: 957–63.

Simons, D.G. and Stevens, M.A. (1972) Scour control in rock basins at culvert outlets, in *River Mechanics*, Vol. II (ed. H.W. Shen), Chapter 24.

Unger, J. and Hager, W.H. (2006) Riprap failure of circular bridge piers, *J. of Hydraulic Engineering*, *ASCE*, 132, No. 4: 354–62.

UPIRI (1940) Technical Memorandum 5, Uttar Pradesh Irrigation Research Institute, Roorkee.

US Army Coastal Engineering Research Center (1984) *Shore Protection Manual*, Washington, DC.

Vittal, N. and Chiranjeevi, V.V. (1983) Open channel transitions: rational method of design. *Journal of the Hydraulics Division, American Society of Civil Engineers*, 109 (1): 99–115.

Watkins, L.H. and Fiddes, D. (1984) *Highway and Urban Hydrology in the Tropics*, Pentech, London.

Yarnell, D.L. (1934) *Bridge Piers as Channel Obstructions*, Technical Bulletin 442, US Department of Agriculture.

Zarrati, A.R. Nazariha, M. and Mashahir, M.B. (2006) Reduction of local scour in the vicinity of bridge pier groups using collars and riprap, *J. of Hydraulic Engineering, ASCE*, 132, No. 2: 154–62.